European Journal of Applied Sciences – Vol. 13, No. 04
Publication Date: September 04, 2025
DOI:10.14738/aivp.1304.19309.
Bamba, B., Koffi, A. K., Soro, S., Kacou, M., Zahiri, É-P., & Bamba, I. (2025). Diurnal Variations of Raindrop Size Distributions in the Tropical Region: Impact on Radar Measurement. *European Journal of Applied Sciences, Vol - 13(04).* 417-438.

Diurnal Variations of Raindrop Size Distributions in the Tropical Region: Impact on Radar Measurement

Bakary Bamba*
Laboratoire des Sciences de la Matière,
de l'Environnement et de l'Energie Solaire,
Université Félix Houphouët-Boigny,
22 BP 582 Abidjan 22, Côte d'Ivoire

Augustin Kadjo Koffi
Laboratoire des Sciences de la Matière,
de l'Environnement et de l'Energie Solaire,
Université Félix Houphouët-Boigny,
22 BP 582 Abidjan 22, Côte d'Ivoire

Séhéna Soro
Laboratoire des Sciences de la Matière,
de l'Environnement et de l'Energie Solaire,
Université Félix Houphouët-Boigny,
22 BP 582 Abidjan 22, Côte d'Ivoire

Modeste Kacou
Laboratoire des Sciences de la Matière,
de l'Environnement et de l'Energie Solaire,
Université Félix Houphouët-Boigny,
22 BP 582 Abidjan 22, Côte d'Ivoire

Éric-Pascal Zahiri
Laboratoire des Sciences de la Matière,
de l'Environnement et de l'Energie Solaire,
Université Félix Houphouët-Boigny,
22 BP 582 Abidjan 22, Côte d'Ivoire

Ibrahima Bamba
Laboratoire des Sciences de la Matière,
de l'Environnement et de l'Energie Solaire,
Université Félix Houphouët-Boigny,
22 BP 582 Abidjan 22, Côte d'Ivoire

ABSTRACT

The diurnal variations of raindrop size distributions (DSDs) observed in tropical Africa (Abidjan, Niamey, Boyélé, Dakar) and South America (Kourou) are analyzed to better understand this variability and its impact on radar measurements. The observed hourly diurnal DSDs display a distinct convex shape, characterized by a

deficit of small drops and a pronounced variation across different daytime periods, particularly in African tropical sites. Local convection is suspected to be the cause of the broader afternoon spectra, whereas the narrower spectra observed in the evening and at night are likely due to organized convective systems, as suggested in the literature. The low diurnal variability of DSDs at the reference site of Kourou may be linked to the typically oceanic nature of precipitation in this region. The hourly diurnal Z=AR^b relationships are not affected by the strong DSD variability at some sites, such as Abidjan. The introduction of a new empirical relationship ($\frac{Z}{D_0/N_T}$) – R proves to be relevant for quantitative precipitation estimation from radar or satellite remote sensing.

Keywords : DSD, Diurnal, Variability, Tropical Africa, Precipitation Estimation.

INTRODUCTION

The issue of climate change, manifested by the increasing frequency of floods and droughts, remains a major concern for the scientific community due to its adverse impacts on populations. As a meteorological parameter that allows us to perceive climate change, rain is a key feature of this study.

In this context, several recent satellite missions, including Megha-Tropiques [1] and Global Precipitation Measurement (GPM) [2], have been launched to better assess the global impact of precipitation on climate and, more importantly, to improve numerical models for quantitative precipitation forecasting. Data from these missions contribute to the effort of reducing the risks associated with extreme rainfall events that affect living conditions, particularly in urban areas. It has been demonstrated that information on raindrop size distribution (DSD) characteristics is essential for establishing empirical relationships among integral rainfall parameters such as the rain rate (R), radar reflectivity factor (Z), median volume diameter (D_0), and total number of drops (N_T). Among these, Z is the parameter used for quantitative rainfall estimation via radar or satellite remote sensing. These remote sensing systems leverage not the directness of their rainfall measurements, but rather their extensive spatial coverage. However, converting reflectivity (Z) into rain rate (R) typically relies on the empirical Z = AR^b relationship, which has been in use since the advent of weather radars. Unfortunately, studies have shown that this relationship varies significantly, regardless of the temporal scale employed [3, 4]. This variability is primarily attributed to the DSD, which directly influences both Z and R.

Consequently, numerous studies have focused on understanding this variability and enhancing radar measurement accuracy. Some authors have suggested that associating a distinct Z = AR^b relationship with each precipitation type (convective or stratiform) could reduce estimation errors [5,6]. However, findings from this approach have been mixed, particularly concerning the values of coefficient A and exponent b in the convective versus stratiform regions of the same squall line. [7] showed that Z–R relationships over land and ocean differ significantly, implicitly highlighting the role of microphysical processes in DSD variability. Other researchers, using data from three co-located disdrometers, have found similar Z–R variations to those observed across different climatic zones.

In a recent study, [4] analyzed the variability of the Z–R relationship at the rainfall occurrence scale and demonstrated the value of simultaneously considering essential DSD parameters particularly drop size (D_0) and number (N_T) through the multicomponent parameter D_0/N_T. When comparing the $Z = AR^b$ and $D_0/N_T = \alpha R^\beta$ relationships, the authors observed that the resulting A–α and b–β associations remained nearly constant, regardless of measurement instruments or precipitation type. This consistency supports the coherence of Z–R variability.

Despite these efforts, the variability of DSD and consequently of the Z–R relationship remains poorly known. Another promising approach involves linking macro-scale precipitation characteristics (convective or stratiform types; isolated or organized structures) with DSD properties. According to [8], such connections are particularly relevant on diurnal and seasonal timescales. Following this perspective, we propose in the present study to analyze the diurnal variations of both DSD and the Z–R relationship in tropical precipitation over Africa and Latin America. Additionally, to improve radar measurement quality, we introduce a new empirical relationship involving the multicomponent parameter $Z/(D_0/N_T)$, inspired by [9], who employed a similar complex parameter Z/D_m.

This work is part of a broader effort to reduce flood risks through a better understanding of diurnal DSD variability and improvement in precipitation estimation from radar or satellite remote sensing. To achieve this, the study pursues two main objectives, focusing on tropical Africa. The first objective is to analyze the diurnal variability of DSD observed in African tropical precipitation, along with that of the empirical Z–R relationship. This diurnal variability will be interpreted in relation to precipitation characteristics (isolated vs. organized systems) and local environmental factors (vegetation cover, topography, ocean–land contrast) specific to each site. The second objective is to introduce a new empirical relationship, $(Z/(D_0/N_T)) - R$, to enhance understanding of Z–R variability and improve the accuracy of radar/satellite precipitation estimates.

To address these objectives, the remainder of the paper is structured as follows: Section 2 describes the datasets and methodology. Section 3 presents and discusses the results. Section 4 summarizes the study and offers concluding remarks.

MATERIALS AND METHODS

Database

The data used in this study consist of historical disdrometer measurements collected at four sites in West Africa (Boyélé, Dakar, Abidjan, and Niamey) and one site in Latin America (Kourou). These datasets have been employed in previous studies, which have confirmed their quality and reliability [10,11,4]. All data were acquired using Joss–Waldvogel Disdrometers (JWD). Table 1 summarizes the main characteristics of the compiled database. In total, it comprises 55994 one-minute raindrop spectra, equivalent to 933 hours and 14 minutes of observation. These measurements cover various climate regimes (coastal Sahelian, coastal equatorial, continental Sahelian, and continental equatorial) thus encompassing different types of precipitation. This diversity allows for a meaningful examination of how local environmental factors relate to the intensity of convective activity and, consequently, their potential effects on the measured DSD characteristics.

Data Processing

The DSD data used in this study were collected using mechanical impact disdrometers (JWDs), which require specific pre-processing due to their susceptibility to contamination. Surface winds can cause the instruments to register spurious signals from non-raindrop particles such as sand grains, plant debris, and bird droppings. Since this type of disdrometer relies on an acoustic impact system that registers any surface impact as a raindrop, precautions must be taken to ensure data quality. To this end, a minimum drop count threshold was applied to validate each one-minute spectrum. A threshold of at least 5 drops per minute was adopted across all study sites except for Dakar, where the following specific minimum values per year were used: 15 (1997), 23 (1998), 18 (1999), and 18 (2000). These thresholds were previously implemented in the works of [10] and [4], where they proved effective in eliminating potentially spurious spectra and improving data reliability.

Sampling of Disdrometer Data

In order to effectively analyze the diurnal variations of DSDs and assess their impact on radar rainfall measurements, we performed a sampling of the disdrometer data by adopting the same hourly classification used by [8]. This approach primarily aims to capture the effects of the diurnal convective cycle on the characteristics of the drop size distribution. The following time intervals were considered:

- Morning DSDs: 00:00–06:00 and 06:00–12:00
- Afternoon and Evening DSDs: 12:00–18:00
- Night time DSDs: 18:00–24:00

To enhance the robustness of the study, the initial dataset (see Table 1) was divided into two subsets. The first subset was used to determine the integrated and analytical parameters of the DSD and to establish mathematical relationships among them with the objective of improving the quantitative estimation of precipitation. This subset is referred to as the "Calibration Dataset". It consists of 52380 one-minute spectra, corresponding to 873 hours of observation (see Table 2), which accounts for approximately 94% of the total data volume, thus ensuring statistical significance and consistency in our results. The second subset, named the "Validation Dataset", was used to verify the results obtained during calibration. Table 3 presents the characteristics of this dataset, which comprises 3614 one-minute rainfall spectra, equivalent to 60 hours and 14 minutes of observation.

It is worth noting that both the calibration and validation datasets were constructed without applying any specific selection criteria regarding the one-minute spectra collected at each site. The integrated parameters are crucial due to their relevance in understanding precipitation in terms that are accessible and comparable across various measurement systems, including rain gauges, disdrometers, weather radars, and satellite sensors. The DSD, typically expressed by the number of drops per unit volume and per diameter interval, denoted N(D), is essential because it provides a functional link to physical quantities that are directly measurable. These include: the total number of drops (NT), the liquid water content (W), the rainfall rate (R), the median volume diameter (D_0), the radar reflectivity factor (Z) and other related integrated parameters. In this study, the DSD analysis method is based on the n-th order statistical moment of the distribution. The n-th order moment, denoted M_n, of the DSD function N(D) is defined by (eq.1):

$$M_n = \int_0^{+\infty} D^n N(D) dD \qquad \text{(eq.1)}$$

To incorporate DSD into radar or satellite rainfall retrieval algorithms, mathematical distribution functions are often used. In this work, we mainly employed the gamma (complete and modified) and lognormal distributions, which are well-suited for modelling DSDs in tropical rainfall regimes (see Table 4).

RESULTS AND DISCUSSION

Observation Sites, Climatology, and Rainfall Regimes

The observation sites considered in this study exhibit diverse geographical and climatic characteristics. Four of them are located in West Africa (Abidjan, Boyélé, Niamey, and Dakar), while one is situated in Latin America (Kourou), as shown in Fig. 1. The average annual rainfall regimes for these sites have been detailed in the work of [12]. These rainfall patterns are markedly variable from one site to another, reinforcing the idea that local factors play a significant role in precipitation dynamics. Overall, both the wet and dry seasons are well-defined across the different locations. While a detailed description of each site's rainfall regime falls outside the scope of this article, we briefly present below the macro-scale factors and sources of precipitation genesis that influence these sites.

A fundamental aspect to consider in understanding the origin of precipitation is the movement of air masses, which are the primary drivers of precipitating systems at both synoptic and local scales. These atmospheric dynamics help explain the prevailing climatic regimes across the study region in the tropics.

To recall, the annual distribution of precipitation in the intertropical zone is closely tied to the position of the meteorological equator, commonly referred to as the Intertropical Convergence Zone (ITCZ). The ITCZ is a low-pressure belt characterized by the convergence of airflows originating from the Southern Hemisphere (the African monsoon flow or south-eastern trade winds) and those from the Northern Hemisphere, known as the Harmattan or north-eastern trade winds. The surface trace of the ITCZ is referred to as the Intertropical Front (ITF), which exhibits seasonal latitudinal shifts.

In addition to this large-scale energetic band, other local factors such as topography, vegetation cover, proximity to water bodies, and the coastal or continental nature of each site also influence rainfall distribution. These factors interact in various proportions, creating heterogeneity in the lower atmosphere, which can modulate the effects of the aforementioned large-scale air masses. They also give rise to small-scale atmospheric phenomena, such as local convection, coastal circulations, and foehn effects, all of which contribute to the complexity and variability of rainfall observed at each site.

Diurnal Variability of DSDs

The diurnal variability of DSDs is illustrated in Fig. 2. To better highlight the differences and similarities between sites, Table 5 presents the characteristic parameters of the mean diurnal DSDs for each location. The key findings are summarized below:

At Abidjan, the mean diurnal DSD during the afternoon and evening period [12:00–18:00] is the broadest, exhibiting a large number of large drops compared to other time intervals (Afternoon: $N_T = 108\ m^{-3}$, $D_0 = 1.76$ mm). It is also characterized by the highest rainfall intensity (Afternoon: R = 3.8 mm·h^{-1}). For all time intervals, the modal drop diameter is approximately 1 mm. In contrast, the mean diurnal DSDs for the evening [18:00–24:00] and morning [00:00–06:00 and 06:00–12:00] are narrower, with the [18:00–24:00] period showing a higher concentration of small drops.

At Niamey, only the afternoon and evening DSD [12:00–18:00] is broad and rich in large drops ($N_T = 118\ m^{-3}$, $D_0 = 2.16$ mm), with the highest rainfall intensity observed during this period (R = 7.0 mm·h^{-1}). Two distinct modal values are observed for all diurnal intervals, around 1 mm and 2 mm. The night-time [18:00–24:00] and morning [00:00–06:00 and 06:00–12:00] DSDs are much narrower, with a deficiency in both small and large drops.

At Dakar, both the morning [00:00–06:00 and 06:00–12:00] and afternoon [12:00–18:00] DSDs are broad, indicating a significant presence of large drops (Morning: $N_T = 95\ m^{-3}$, $D_0 = 1.80$ mm; Afternoon: $N_T = 74\ m^{-3}$, $D_0 = 1.78$ mm). These intervals exhibit higher rainfall intensities compared to the night-time DSD [18:00–24:00], which is the narrowest, with a marked lack of both small and large drops (Night: R = 1.7 mm·h^{-1}; Morning: R = 3.3 mm·h^{-1}). Modal drop diameters are around 1 mm, and no DSD exceeds 4 mm in drop size.

At Boyélé, the mean DSDs during the morning [06:00–12:00] and afternoon [12:00–18:00] are also broad, indicating a strong presence of large drops (Morning: $N_T = 79\ m^{-3}$, $D_0 = 2.10$ mm; Afternoon: $N_T = 74\ m^{-3}$, $D_0 = 2.00$ mm), with the highest average rainfall intensities recorded during these times (Afternoon: R = 2.9 mm·h^{-1}; Morning: R = 4.0 mm·h^{-1}). Modal drop size is around 1 mm. The early morning DSD [00:00–06:00] is very narrow, indicating an absence of large drops.

At Kourou, diurnal DSDs are generally broad, except during the afternoon [12:00–18:00], which is noticeably narrow and deficient in large drops. However, this interval appears to have a higher number of small drops, with an intensity comparable to that of the morning DSD [06:00–12:00]. As in Dakar, drop diameters rarely exceed 4 mm.

These findings clearly illustrate the diurnal variability of DSDs observed in tropical rainfall over Africa and Latin America. However, this diurnal variability is more pronounced in tropical African sites, especially in the area of large drops. This result aligns with the findings of [8]. A detailed analysis reveals that the studied sites can be categorized based on the dominance of small-scale atmospheric phenomena (local convection, coastal circulation, ocean-land contrast, or foehn effects) versus large-scale systems (anticyclones, organized convective systems).

- The first group, comprising Abidjan and Niamey, is characterized by broad afternoon DSDs [12:00–18:00] with abundant large drops. This can be attributed to intense local convection over land, which is known to be active in the afternoon and evening, favoring the coalescence process. Previous studies [11, 8] have associated this with elevated sea surface temperatures (SST) or localized convective activity. By contrast, the night [18:00–24:00] and morning [00:00–12:00] DSDs in this group are narrower, likely linked to organized convective systems such as squall lines [13], where breakup processes dominate. These findings suggest that the diurnal DSD behaviour at these sites is comparable to those in tropical Asia.

- The second group, represented by Boyélé, shows broad DSDs in both the morning [06:00–12:00] and afternoon [12:00–18:00], indicating that local convection may start earlier in the day at this site. The very narrow early morning DSD [00:00–06:00] is attributed to organized systems, while the evening DSD [18:00–24:00] appears to result from a combination of local convection and organized convection.
- The third group, Dakar, features broad DSDs throughout the day, including the morning, likely influenced by both local convection and trailing stratiform rainfall from squall lines. According to [14], convective storms (isolated thunderstorms and squall lines) are the only sources of rainfall in Dakar. The prevailing mechanism for DSD formation here is coalescence, while the narrow night-time DSD results from breakup processes within the convective parts of squall lines.
- The fourth group, Kourou, is considered a reference site in this study. It shows minimal diurnal variation in DSDs, except for a deficiency in drops sized between 3 mm and 4 mm. As noted by [8], this weak variability may stem from the predominantly oceanic nature of the convective precipitation at this coastal-equatorial site. Nonetheless, the broad morning and night DSDs could be associated with local oceanic convection or stratiform precipitation driven by coastal circulation or the foehn effect both linked to the coalescence process. Conversely, the narrow afternoon DSD may suggest that continental convection inhibits coalescence, promoting drop breakup instead.

ADJUSTMENT OF OBSERVED DIURNAL DSD

To effectively integrate the analysis of the diurnal variability of the Drop Size Distribution (DSD) presented earlier into rainfall estimation algorithms, we fitted the observed diurnal spectra using several analytical distribution functions commonly used for modelling tropical rainfall DSDs, namely the log-normal and gamma distributions. Indeed, the observed diurnal DSDs are well represented by these forms, as confirmed by findings widely reported in the literature.

Fig. 3-A-B, 3-C-D, and 3-E clearly show that the gamma functions (both modified and complete), as well as the log-normal distribution, adequately reproduce the observed mean diurnal DSDs for all the studied sites. However, this fitting exercise performed qualitatively without calculating the mean square error reveals that the most suitable model varies depending on the climatic zone considered. To support this qualitative choice, **Table 6** presents the average fitting parameters for the different models, allowing a direct comparison with observed parameters.

- Abidjan Site*:* At the coastal site of Abidjan, the modified gamma distribution tends to overestimate small drops, while the complete gamma function underestimates large drops. Conversely, the log-normal model fits both small and large drops effectively. Therefore, the log-normal distribution is the most appropriate for representing the diurnal DSDs at this site. Its associated parameters $\mathbf{D_g}$ (characteristic drop size), $\mathbf{N_T}$ (total drop count), and $\boldsymbol{\sigma}$ (spectral width) can be directly used in rainfall estimation algorithms. This choice is validated by the high value of D_g (D_g = 1.12 mm) observed for the wide diurnal DSDs in the afternoon and evening, as previously mentioned.
- Niamey Site*:* At the Sahelian site of Niamey, both gamma distributions (especially the complete version) provide the best fit to the observed diurnal spectra, accurately capturing both small and large drops. The log-normal function, however, poorly

represents large drops. As a result, the gamma model is deemed most suitable for this site. Its parameters $\mathbf{D_m}$ (mean drop diameter), $\mathbf{N_T}$, and $\boldsymbol{\mu}$ (spectral shape) are recommended for use in rainfall estimation algorithms. The high value of D_m (D_m = 2.1 mm) observed for the wide afternoon and evening DSDs further supports this choice.

- Boyélé Site*:* The results from Boyélé are similar to those observed at Niamey. Only the gamma functions, particularly the complete version, correctly fit the observed diurnal DSDs. Therefore, the gamma distribution is the most appropriate analytical model for representing the diurnal DSDs at this equatorial continental site. **Table 5** confirms this, with high D_m values observed for the morning (6:00–12:00) and afternoon DSDs (D_m = 2.1 mm in both cases), which are considered wide.
- Dakar Site*:* Dakar shares similarities with Abidjan in terms of DSD fitting. The log-normal model accurately represents the mean diurnal DSDs observed at this site, for both small and large drops. Moreover, the highest Dg values are recorded during the morning (D_g = 1.12 mm) and afternoon (D_g = 1.13 mm), confirming the presence of wide DSDs during these periods.
- Kourou Site*:* Like the Niamey and Boyélé sites, the diurnal DSDs observed at Kourou are best represented by the gamma functions especially the complete version. This is clearly evidenced by the high D_m values for the wide DSDs recorded in the morning (D_m = 1.61 mm) and at night (D_m = 1.69 mm)

This study, based on the fitting of observed diurnal DSDs, allowed us to assign a specific analytical form to each diurnal DSD as well as to each studied climatic zone. It also confirmed the existence of diurnal variability in the DSD.

Relevance of the Study

To further highlight the necessity of studying DSDs at the diurnal scale, Fig. 4 presents the overall mean diurnal DSD superimposed on the four average hourly diurnal DSDs analyzed. This comparison yields very satisfactory results, supporting the relevance of investigating DSDs on a diurnal basis. Indeed, this type of study holds considerable value, as extreme weather events (such as floods and droughts) generally occur on a diurnal timescale, which closely aligns with the scale of individual rainfall events. Moreover, these phenomena are more perceptible at this temporal resolution.

That is why, in this work, we aim to determine whether a quantitative assessment of rainfall at the event scale considered globally (i.e., regardless of the hourly classes) might introduce additional errors when estimating rainfall at diurnal time intervals. Accordingly, the analysis of Fig. 4 reveals results that vary depending on the climatic zone.

For the sites of Abidjan and Niamey, the overall mean diurnal DSD underestimates the mean diurnal DSD of the afternoon and evening [12:00–18:00], while it overestimates the mean diurnal DSDs of the night [18:00–24:00] and early morning [00:00–06:00]. However, it accurately reproduces the mean diurnal DSD of the late morning [06:00–12:00].

At Boyélé, the mean diurnal DSD of the night [18:00–24:00] is very well represented, while the early morning DSD [00:00–06:00] is overestimated, and those of the late morning [06:00–12:00] and afternoon [12:00–18:00] are underestimated.

For the Dakar site, the overall mean diurnal DSD closely matches the mean diurnal DSD of the afternoon and evening [12:00–18:00], but it significantly overestimates the night DSD [18:00–24:00] and underestimates those of the early and late morning [00:00–06:00 and 06:00–12:00]. At Kourou, the overall mean diurnal DSD accurately reflects all the mean hourly diurnal DSDs, regardless of drop size. Such a result is linked to the low diurnal variability of DSDs observed at this site. However, the overall mean diurnal DSD shows some difficulty in representing the afternoon and evening mean diurnal DSD [12:00–18:00], particularly around raindrops with a diameter of 3 mm.

This work demonstrates that measuring rainfall at the scale of the entire rain event or at a broader scale (day, month, year) can introduce additional sources of error in the quantitative estimation of precipitation using radar/satellite remote sensing. A credible alternative would be to consider diurnal time intervals, as proposed by [8], and as adopted in this study. However, this approach is particularly relevant for climatic zones that exhibit significant diurnal variability, as clearly observed across the various tropical African sites studied here. In this regard, local convection over land and organized convective systems both key drivers of strong diurnal DSD variability through their distinctive signatures in the width (narrow or broad) of the diurnal rainfall spectra should also be integrated at this diurnal scale into precipitation simulation models.

Impact of Diurnal DSD Variations on Radar Rainfall Measurement
Case of the Z-R Relationship:

As previously mentioned, one major source of uncertainty in the quantitative estimation of precipitation from radar/satellite remote sensing is the diurnal variability of the Drop Size Distribution (DSD**).** To better understand this, we focus here on the Z-R relationship**.** Based on disdrometer observations, the most common and simplest method to determine the Z-R relationship is that introduced by **[3]**, resulting in the general form: $Z = AR^b$**.**

In this study, the determination of the coefficient **A** and the exponent **b** of the Z-R relationship was performed using the least squares method on calibration data (see Table 2). Fig. 5-a-b, 5-c-d, and 5-e show the scatter plots of the (Z, R) pairs as well as their corresponding fitted curves and associated equations for the individual diurnal hourly classes [00:00–06:00], [06:00–12:00], [12:00–18:00], and [18:00–24:00] across the various study sites (Abidjan, Niamey, Dakar, Boyélé, and Kourou). As can be seen in the graphs, the power-law form of the Z-R relationship is well captured, as the correlation coefficients are all close to one. Table 7 summarizes the diurnal Z-R relationships derived from the various hourly precipitation samples observed at the aforementioned sites. Based on the analysis of Table 7 and Fig. 5-a-b, 5-c-d, and 5-e, the following key findings emerge:

- The low diurnal variability of DSDs at the reference site Kourou is clearly reflected in the stability of its diurnal Z-R relationships**.** The average diurnal Z-R relationship for Kourou can be expressed as $Z = 202R^{1.3}$.

Surprisingly**,** Abidjan and Dakar, despite exhibiting strong diurnal DSD variability, also display stable diurnal Z-R relationships without significant differences. The hourly diurnal Z-R relationships for these two sites can be simplified into the following mean diurnal expressions: Abidjan : $Z = 340R^{1.3}$, Dakar : $Z = 321R^{1.3}$.

At Niamey, the pronounced diurnal variability of DSDs results in Z-R relationships that show clear and significant differences**.** For instance, the DSDs of the morning periods ([00:00–06:00] and [06:00–12:00]) and the afternoon period ([12:00–18:00]) have similar Z-R relationships, allowing them to be represented by the following mean relation: $Z = 514R^{1.3}$. Meanwhile, the evening DSD ([18:00–24:00]) is better represented by: $Z = 463R^{1.3}$.

- Similarly, Boyélé, with its notable diurnal DSD variability, shows marked differences in its diurnal Z-R relationships. For example, the morning ([06:00–12:00]) and afternoon ([12:00–18:00]) periods have nearly identical Z-R relationships, represented by: $Z = 346R^{1.4}$. The night and early morning periods ([00:00–06:00] and [18:00–24:00]), which also show similar Z-R behavior, are best described by: $Z = 397R^{1.3}$.
- The analysis of Figures 5-a-b, 5-c-d, 5-e, and Table 7 also reveals that the highest values of the coefficient A in the diurnal Z-R relationships are observed at Niamey, while the lowest values are found at Kourou. Abidjan, Dakar, and Boyélé exhibit moderate A values. These specificities in the diurnal Z-R relationship can likely be explained by the precipitation formation mechanisms. For example, Niamey's rainfall is primarily generated by local continental convection and organized convective systems, whereas Kourou's rainfall mostly originates from oceanic sources. Sites such as Abidjan, Dakar, and Boyélé receive rainfall from both continental and oceanic convective sources (particularly for Abidjan and Dakar). They are also influenced by mesoscale convective systems (e.g., squall lines) and occasionally stratiform rain resulting from foehn effects.

This study demonstrates that using the Z-R relationship alone is not always suitable for investigating the diurnal variability of DSDs, as it may obscure certain DSD fluctuations particularly at stations where rainfall arises from diverse sources (e.g., local convection, foehn effect, ocean-land contrasts, mesoscale convective systems).

Case of the Z-R Relation Parameterized by D_0/N_T:

The diurnal variations in the integral and analytical parameters highlighted above naturally introduce constraints in any attempt to develop generalized empirical relationships between such parameters e.g., D_0–R, N_T–R, Z–R, W–R, and more recently (D_0/N_T) –R, as introduced by [4]. Given that the precipitation observed at the various tropical sites under study is generally convective in origin, these constraints stem from diverse microphysical processes such as coalescence, breakup, and updrafts/downdrafts that govern the diurnal characteristics of the DSD [15,16].

For this reason, [4] demonstrated that the drop size (D_0) and drop number concentration (N_T) which characterize the DSD and represent the net result at ground level of all microphysical processes can be more effectively considered together using the parameter D_0/N_T**.** This combined parameter helps explain the variability in the Z–R relationship. These authors developed a simple empirical relationship of the form (D_0/N_T) –R**,** analogous to the traditional Z–R formulation, and showed that its coefficients could be used to control or adjust the parameters of the Z–R relationship.

[17] further showed that empirical relationships involving only one integral parameter (D_0 or N_T) do not always yield accurate rainfall retrievals. Therefore, in this study, we focused on the complex integral parameter D_0/N_T, considered a more direct indicator of the underlying

microphysical processes, to build a new empirical relationship. This relationship is based on the multi-complex parameter $Z/(D_0/N_T)$, which essentially normalizes Z by D_0/N_T.

Fig. 6-a-b, 6-c-d, and 6-e present the scatter plots of the pair ($Z/(D_0/N_T)$, R), along with the corresponding fitted curves and relationships for each diurnal time class: [00:00–06:00], [06:00–12:00], [12:00–18:00], and [18:00–24:00], across the different study sites (Abidjan, Niamey, Dakar, Boyélé, and Kourou).

As observed in the plots, the shape of the fitted curves is similar to the power-law form of the $Z = AR^b$ relationship. However, in terms of comparing the effectiveness of R estimation, the results from the Z–R and $Z/(D_0/N_T)$–R relationships are compiled in Table 8. Analysis clearly shows that for all individual diurnal time classes, the correlation coefficients follow this order:

$$\mathbf{r\,[Z/(D_0/N_T)–R] > r\,[Z–R].}$$

It is also noted that, throughout the different diurnal phases of rainfall, the pre-factor of the $Z/(D_0/N_T)$–R relationship systematically varies, while the exponent remains nearly constant for a given site. This finding is especially interesting as it shows that, compared to the traditional Z–R relationship, the new formulation better captures the diurnal variability of DSD previously described.

Therefore, the empirical $Z/(D_0/N_T)$–R relationship stands out as the best alternative to replace the traditional Z–R relationship in the challenging task of rainfall rate estimation using polarimetric radars or Doppler profilers which can measure multiple variables such as Z, Z_{DR}, and K_{DP}, used to derive D_m and N_T. The multi-complex parameter to be used in radar algorithms could then be expressed as $Z/(D_m/N_T)$, which is analogous to $Z/(D_0/N_T)$.

Validation of the $Z/(D_0/N_T)$ – R Relationship:

To validate the $Z/(D_0/N_T)$ – R relationship, considered superior to the traditional Z–R relationship for quantitative precipitation estimation using radar/satellite remote sensing, two approaches can be employed:

1. The first consists of calculating the parameters Z, D_0, and N_T from DSD data obtained by a disdrometer, then reconstructing the rainfall rate R using the empirical $Z/(D_0/N_T)$ – R relationship. This estimated R is then compared to the actual rainfall rate directly measured by the disdrometer.
2. The second approach is based on the use of an independent validation dataset, these data were not used in developing the $Z/(D_0/N_T)$ – R equation.

In this study, we adopted the second approach, by constructing scatter plots of the two parameters [$Z/(D_0/N_T)$, R] using validation data, and then superimposing the fitted curve previously obtained from the calibration dataset. This exercise was conducted for several diurnal time classes at different sites. The resulting plots are shown in Fig. 7. Analysis of these plots shows that the scatter points are well dispersed around the fitted curves, indicating a strong agreement between observed and estimated values. This result confirms that the new empirical $Z/(D_0/N_T)$ – R relationship does indeed lead to an improvement in quantitative precipitation estimation compared to the conventional Z–R relationship.

Other researchers have also used multi-complex parameters in rainfall retrieval efforts, achieving highly satisfactory results. For example, [9] used the Z/Dm multi-complex parameter and were able to enhance rainfall rate estimation compared to the Z–R relationship. Likewise, [17], through their approach involving normalization by N_0***,** demonstrated a significant improvement in correlation coefficients from 0.84 to 0.98 and a reduction in standard deviation from 0.26 to 0.12 in rainfall retrieval accuracy.

CONCLUSION

In this study, we investigated the diurnal variations of raindrop size distributions (DSDs) and examined their impact on radar measurements. Specifically, the study demonstrated that diurnal variability in DSDs is linked to phenomena such as local convection, mesoscale convective systems, and local factors (e.g., ocean–land contrast, vegetation, topography). This analysis aligns with the perspective of [8].

Our primary objective was to contribute to highlighting the diurnal variability of DSDs and to propose a new empirical relationship based on a multi-complex integrated parameter, as opposed to the simple integrated parameters commonly used in the literature.

The investigation of diurnal DSD variability revealed significant differences, both between hourly time slots and across different tropical sites. For the tropical African sites (Abidjan, Niamey, Dakar, and Boyélé), average DSDs observed during the afternoon and evening [12:00–18:00] tended to have broader shapes, indicative of a high presence of large drops, while those during the night [18:00–24:00] had narrower profiles. Local convection, local factors, and organized convective systems were suspected as the likely causes, consistent with the findings of [13]and [8]. In contrast, Kourou (located on the northeast coast of South America) showed the least diurnal variation, likely due to the purely oceanic origin of precipitation in that region. Analysis of DSD characteristics (D_0, N_T) confirmed the broad and narrow configurations highlighted by the diurnal DSD profiles.

Efforts to fit adjustment models to each observed diurnal DSD at the various sites were successful. The log-normal model was chosen for Abidjan and Dakar, while the gamma distribution was better suited for Niamey, Boyélé, and Kourou.

The analysis of the usefulness of diurnal-scale DSD analysis showed that, for tropical African sites with strong diurnal variability, replacing an hourly-specific diurnal DSD with a global diurnal mean introduces additional errors, as the latter cannot accurately represent all hourly DSD profiles. The evaluation of how diurnal DSD variations affect radar measurements, using the empirical Z–R relationship, showed that the impact is not always clear. For example, at Abidjan, the hourly Z–R relationship was found to be nearly constant, suggesting that the traditional Z–R relation does not always capture key information about DSD diurnal variability particularly at sites where precipitation has diverse origins (local convection, foehn effect, ocean–land contrast, mesoscale convective systems).

On the other hand, the use of a multi-complex integrated parameter, $Z/(D_0/N_T)$, to introduce a new empirical relationship, $Z/(D_0/N_T) - R$, produced satisfactory results. Indeed, we showed that this new relationship accurately reflects the diurnal variability of DSDs and yields higher correlation coefficients compared to the traditional Z–R relationship. As such, it can be considered a viable alternative for quantitative rainfall retrieval from radar/satellite observations, consistent with the findings of Sharma et al. (2009) [9] for the Z/D_m – R relationship.

Future perspectives of this work could include:

- Extending the same type of study, based on the same (or other) disdrometer datasets, by considering specific rain types (e.g., stratiform: 3 mm/h; convective: 30 mm/h), and also different rainy seasons, as was done by [8] in Asia (Kototabang, Gadanki, and Singapore).
- Conducting joint analyses using DPR satellite data and recent disdrometer observations, in order to explore the relationship between diurnal variability in the new $Z/(D_0/N_T)$ – R empirical relationship and the underlying microphysical processes.

ACKNOWLEDGMENTS

The authors are grateful to all of those who contributed to the data set used in this study, especially to Prof. H. Sauvageot who initiated EPSAT program and contributed strongly for the extension of the experiment to Abidjan (Côte d'Ivoire).

References

[1] R. Roca, H. Brogniez, P. Chambon, O. Chomette, S. Cloché, M. E. Gosset, J.-F. Mahfouf, P. Raberanto and N. Viltard, The Megha-Tropiques mission : a review after three years in orbit. (2015), *Front. Earth Sci.*, vol. 3, pp. 1–14.

[2] A. Y. Hou, R. K. Kakar, S. Neeck, A. A. Azarbarzin, and D. Christian, The Global Precipitation Measurement (GPM) Mission, *Bull. Am. Meteorol. Soc.* (2008), vol. 95, pp. 701–722.

[3] J. S. Marshall and W. M. K. Palmer, The Distribution of Raindrops with Size, *Journal of the Atmospheric Sciences*. (1948), vol. 5(4), pp. 165-166.

[4] A. D. Ochou, E.-P. Zahiri, B. Bamba and M. Koffi. Understanding the Variability of Z-R Relationships Caused by Natural Variations in Raindrop Size Distributions (DSD) : Implication of Drop Size and Number. *Atmospheric and Climate Sciences*. (2011), vol. 1, pp. 147-164 https://doi.org/10.4236/acs.2011.13017.

[5] H. Sauvageot and J. P. Lacaux, The shape of averaged drop size distributions, *J. Atmos. Sci.* (1995) vol. 52, pp. 1070-1083.

[6] M. Maki, T. D. Keenan, Y. Sasaki and K. Nakamura, Characteristics of the Raindrop Size Distribution in Tropical Continental Squall Lines Observed in Darwin, Australia. *Journal of Applied Meteorology and Climatology*, (2011), vol. *40*(8), pp. 1393-1412.

[7] R. S. Tenório, M. C. da S. Moraes and H. Sauvageot, Raindrop Size Distribution and Radar Parameters in Coastal Tropical Rain Systems of Northeastern Brazil, *Journal of Applied Meteorology and Climatology*. (2012), vol. 51(11), pp. 1960-1970.

[8] T. Kozu, Z. Akramin, T. Shimomai, S. Mori, H. Hashiguchi, Y. Shibagaki, Y. N. Takayabu and S. Saraspriya,). Seasonal, Intra-Seasonal and Diurnal Variations of Raindrop Size Distribution at Koto Tabang, West Sumatra. The 2nd TRMM International Science (2005)

[9] S. Sharma, M. Konwar, D. Sarma, M. Kalapureddy and A. Jain, Characteristics of Rain Integral Parameters during Tropical Convective, Transition, and Stratiform Rain at Gadanki and Its Application in Rain Retrieval, *Journal of Applied Meteorology and Climatology*. (2009), vol. 48, pp. 1245-1266.

[10] B. Bamba, A. D. Ochou, E.-P. Zahiri, and M. Kacou, Consistency in Z-R Relationship Variability Regardless Precipitating Systems, Climatic Zones Observed from Two Types of Disdrometer, *Atmospheric and Climate Sciences*. (2014), vol. 4 (5), pp. 941-955.

[11] B. Bamba, E.-P. Zahiri, M. Kacou, A. D. Ochou, Y. Kouadio, I. Bamba, A. K. Koffi, Seasonal variability of raindrop size distributions characteristics regarding to climatic parameters over coastal area of West Africa, *International Journal of Innovation and Scientific Research*. (2020), vol. 49(1), pp.75-88.

[12] A. D. Ochou, Variabilité spatio-temporelle des moments statistiques des distributions de gouttes de pluie et conséquences sur la mesure des précipitations par télédétection micro-ondes, *PhD Thesis, Université Cocody Abidjan*. (2003), 185 p.

[13] S. Mori, H. Jun-Ichi, Y. I. Tauhid, M. D. Yamanaka, N. Okamoto, F. Murata, N. Sakurai, H. Hashiguchi and T. Sribimawati, Diurnal Land–Sea Rainfall Peak Migration over Sumatera Island, Indonesian Maritime Continent, Observed by TRMM Satellite and Intensive Rawinsonde Soundings. *Monthly Weather Review*. (2004), vol. 132(8), pp. 2021-2039.

[14] B. Bamba, A. D. Ochou, E.-P. Zahiri, and M. Kacou, Consistency in Z-R Relationship Variability Regardless Precipitating Systems, Climatic Zones Observed from Two Types of Disdrometer, *Atmospheric and Climate Sciences*. (2014), vol. 4 (5), pp. 941-955.

[15] G. W. Lee, I. Zawadzki, W. Szyrmer, D. Sempere-Torres and R. Uijlenhoet, A General Approach to Double-Moment Normalization of Drop Size Distributions. *Journal of Applied Meteorology and Climatology*. (2004), vol. *43*(2), pp. 264-281.

[16] D. Rosenfeld and C. W. Ulbrich, Cloud microphysical properties, processes, and rainfall estimation opportunities, Radar and Atmospheric Science : A collection of essays in honor of David Atlas, *Meteor. Monogr.* (2003), vol. 30, pp. 237-258.

[17] J. Testud, S. Oury, R. A. Black, P. Amayenc and X. Dou, The Concept of “Normalized” Distribution to Describe Raindrop Spectra : A Tool for Cloud Physics and Cloud Remote Sensing. *Journal of Applied Meteorology and Climatology*. (2001), vol. *40*(6), pp. 1118-1140.

List of Tables

Table 1: Acquired disdrometric database

Sites	Geographic Coordinates	Measurement Period	DSD de 1 minute
Abidjan (Côte d'Ivoire)	5°25 N, 4° W	1986 (juin ; sept-Oct. Nov-déc) 1987 (janv. à déc.) 1988 (janv. à juin)	17041
Niamey (Niger)	13°30 N, 2°10 E	1989 (juil-août-sept)	3135
Dakar (Sénégal)	14,72° N, 17,47° W	1997 (Juil. -Oct.) 1998(Juil. -Sept.) 1999(Juil. -Sept.) 2000(Juil.-Oct.)	14586
Kourou (Guyane)	4°N, 52°W	1991 (avr-mai ; juil.-août-sept)	7112
Boyélé (Congo)	2°50 N, 18°04 E	1988 (mai-juin-juil. ; sept-Oct. Nov-déc) 1989 (mars-avr.-mai-juin)	14120

Table 2: Calibration Data

Sites	DSD de 1 minute
Abidjan (Côte d'Ivoire)	16506
Niamey (Niger)	2773
Dakar (Sénégal)	13666
Kourou (Guyane)	6592
Boyélé (Congo)	12843

Table 3: Validation Data

Sites	DSD de 1 minute
Abidjan (Côte d'Ivoire)	535
Niamey (Niger)	362
Dakar (Sénégal)	920
Kourou (Guyane)	520
Boyélé (Congo)	1277

Table 4: The Adjustment functions used

NAME	FORMULE
Modified Gamma distribution function (Ulbrich, 1983)	$N(D) = N_0 D^{\mu} \exp(-\Lambda D)$
Full Gamma distribution function **(**Chandrasekar et Bringi (1987)	$N(D) = N_T \dfrac{\Lambda^{\mu+1}}{\Gamma(\mu+1)} D^{\mu} \exp(-\Lambda D)$

Log normal distribution function Feingold et Levin (1986)	$N(D)=\frac{N_T}{\sqrt{2\pi}D\ln\sigma}\exp\left[-\frac{\ln^2(D/D_g)}{2\ln^2\sigma}\right]$

Table 5: Characteristic Parameters of Observed average daytime DSDs

		Paramètres moyens DSD horaires observées							
	Paramètres DSD Classes Horaires	**R (mm.h-1)**	**W (gm-3)**	**Z (dBZ)**	**(m-3)**	**(mm)**	**(mm)**	**(mm.m3)**	**x (mm.m-3)**
ABIDJAN	24h00-06h00	2,92	141	32,88	104,88	1,60	1,64	15	167,81
	06h00-12h00	3,30	157	34,02	110,87	1,68	1,72	15	186,26
	12h00-18h00	3,79	175	35,27	107,83	1,76	1,82	16	189,78
	18h00-24h00	2,38	116	31,97	91,32	1,60	1,64	18	146,11
NIAMEY	24h00-06h00	3,52	0,15	35,66	66,94	2,03	2,05	30	135,88
	06h00-12h00	4,56	0,20	37,06	102,17	1,99	2,04	19	203,32
	12h00-18h00	7,22	0,30	39,59	118,41	2,16	2,21	18	255,77
	18h00-24h00	5,18	0,22	37,37	96,75	2,08	2,07	21	201,24
DAKAR	24h00-06h00	3,34	154	34,01	94,76	1,80	1,78	19	170,57
	06h00-12h00	3,15	145	34,12	92,83	1,76	1,77	19	163,38
	12h00-18h00	2,58	120	32,60	74,46	1,78	1,74	24	132,54
	18h00-24h00	1,72	84	30,18	63,92	1,61	1,62	25	102,91
BOYELE	24h00-06h00	2,06	97	31,61	78,44	1,78	1,72	23	139,62
	06h00-12h00	3,98	133	35,65	79.32	2,06	2,10	26	163,40
	12h00-18h00	2,89	124	35,38	74,46	2,03	2,09	27	151,15
	18h00-24h00	2,39	106	34,20	67,84	1,95	2,00	29	132,29
KOUROU	24h00-06h00	2,04	0,10	31,27	136,32	1,54	1,60	11	209,93
	06h00-12h00	2,67	0,13	32,47	161,20	1,59	1,61	10	256,31
	12h00-18h00	2,52	0,13	30,81	194,48	1,42	1,44	7	276,16
	18h00-24h00	1,81	0,09	32,05	117,99	1,55	1,69	13	182,88

Table 6: Characteristic analytical Parameters of average daytime DSDs fitted by Lognormal, full Gamma and modified Gamma functions.

	Paramètres DSDs Classes Horaires	**Log-Normale LogN**			**Gamma Complète GamC**			**Gamma Modifié GamM**			
		(mm)	**(m-3)**		**(mm-1)**	**(m-3)**		**(mm)**		**(mm-1)**	
ABIDJAN	24h00-06h00	1,07	104,88	1,41	7,04	104,88	7,03	1,64	2803,9	3,19	1,24
	06h00-12h00	1,06	110,87	1,45	5,86	110,87	5,67	1,72	2160,4	2,91	1,00
	12h00-18h00	1,12	107,83	1,44	5,82	107,83	5,96	1,82	1757,9	2,72	0,96
	18h00-24h00	1,02	91,32	1,45	6,07	91,32	5,64	1,64	2364	3,23	1,29
DAKAR	24h00-06h00	1,11	94,76	1,46	5,54	94,76	5,62	1,78	2704,7	3,26	1,78
	06h00-12h00	1,12	92,83	1,43	6,05	92,83	6,21	1,77	1771,8	2,85	1,04
	12h00-18h00	1,13	74,46	1,43	6,06	74,46	6,30	1,74	2579,2	3,41	1,94
	18h00-24h00	1,05	63,92	1,42	6,87	63,92	6,72	1,62	2522,4	3,59	1,81
NIAMEY	24h00-06h00	0,93	78,44	1,57	4,34	78,44	3,48	1,72	2045,4	3,37	1,82
	06h00-12h00	0,95	79,32	1,67	3,06	79,32	2,32	2,10	784,9	2,56	1,39
	12h00-18h00	0,95	74,46	1,67	3,05	74,46	2,31	2,09	711,5	2,50	1,21
	18h00-24h00	1,17	96,75	1,55	3,62	1,17	3,67	2,07	1800,1	2,93	2,06
BOYELE	24h00-06h00	0,93	78,44	1,57	4,34	78,44	3,48	1,72	2045,4	3,37	1,82
	06h00-12h00	0,95	79,32	1,67	3,06	79,32	2,32	2,10	784,9	2,56	1,39
	12h00-18h00	0,95	74,46	1,67	3,05	74,46	2,31	2,09	711,5	2,50	1,21

	18h00-24h00	0,96	67,84	1,61	3,52	67,84	2,82	2,00	699,9	2,52	1,03
KOUROU	24h00-06h00	0,72	136,32	1,66	4,12	136,32	2,37	1,6	1855,2	3,07	0,91
	06h00-12h00	0,75	161,20	1,66	4,01	161,20	2,41	1,61	2500,4	3,12	1,04
	12h00-18h00	0,73	194,48	1,62	4,75	194,48	2,87	1,44	6409,8	3,87	1,57
	18h00-24h00	0,72	117,99	1,65	4,21	117,99	2,46	1,69	701,7	2,34	-0,05

Table 7: Diurnal Z-R relationships obtained at differents measurement sites.

Sites	Hourly classes	Relation Z-R (Z=ARb)	Correlation Coefficient r
ABIDJAN	24H-06H	Z=316,9R1,30	0,98
	06H-12H	Z=333,8R1,28	0,98
	12H-18H	Z=348,7R1,26	0,98
	18H-24H	Z=358,4R1,28	0,98
DAKAR	24H-06H	Z=341,9R1,28	0,98
	06H-12H	Z=323,6R1,30	0,98
	12H-18H	Z=308,8R1,27	0,98
	18H-24H	Z=310,8R1,31	0,98
NIAMEY	24H-06H	Z=513,3R1,22	0,97
	06H-12H	Z=517,6R1,35	0,98
	12H-18H	Z=512,4R1,35	0,98
	18H-24H	Z=462,6R1,28	0,97
BOYELE	24H-06H	Z=412,2R1,36	0,98
	06H-12H	Z=328,7R1,40	0,98
	12H-18H	Z=363,9R1,36	0,98
	18H-24H	Z=382,5R1,33	0,98
KOUROU	24H-06H	Z=202,6R1,35	0,99
	06H-12H	Z=214,8R1,36	0,98
	12H-18H	Z=194,5R1,32	0,99
	18H-24H	Z=194,5R1,35	0,98

Table 8 : Comparison of correlation coeffcients empirical Z-R and $Z_{rapport}$-R relationships of differents diurnal hourly classes studied.

	Relations Hourly classes	Relation Z-R (Z=ARb)	Correlation coefficient r	Relation Zrapport-R (Z=)	Correlation coefficient r
ABIDJAN	24H-06H	Z=316,9R1,30	0,98	Z=9452,8R1,71	0.99
	06H-12H	Z=333,8R1,28	0,98	Z=8564,1R1,73	0,99
	12H-18H	Z=348,7R1,26	0,98	Z=8056,2R1,75	0,99
	18H-24H	Z=358,4R1,28	0,98	Z=8247,8R1,73	0,99
DAKAR	24H-06H	Z=341,9R1,28	0,98	Z=10898,2R1,68	0,99
	06H-12H	Z=323,6R1,30	0,98	Z=11161,5R1,67	0,99
	12H-18H	Z=308,8R1,27	0,98	Z=11342,0R1,71	0,99
	18H-24H	Z=310,8R1,31	0,98	Z=10105,6R1,68	0,99
NIAMEY	24H-06H	Z=513,3R1,22	0,97	Z=8948,9R1,64	0,98
	06H-12H	Z=517,6R1,35	0,98	Z=6981,9R1,66	0,98
	12H-18H	Z=512,4R1,35	0,98	Z=6707,8R1,63	0,99
	18H-24H	Z=462,6R1,28	0,97	Z=8282,0R1,63	0,99
BOYELE	24H-06H	Z=412,2R1,36	0,98	Z=10587,5R1,59	0,99
	06H-12H	Z=328,7R1,40	0,98	Z=13129,4R1,52	0,99
	12H-18H	Z=363,9R1,36	0,98	Z=11377,4R1,57	0,99
	18H-24H	Z=382,5R1,33	0,98	Z=10270,3R1,60	0,99

KOUROU	24H-06H	Z=202,6R1,35	0,99	Z=19762,4R1,56	0,99
	06H-12H	Z=214,8R1,36	0,98	Z=16938,1R1,58	0,99
	12H-18H	Z=194,5R1,32	0,99	Z=18185,8R1,59	0,99
	18H-24H	Z=194,5R1,35	0,98	Z=18445,4R1,58	0,99

$$Z_{rapport} = \frac{Z}{D_0/N_T}$$

List of Figure

Fig. 1: Location of studies sites

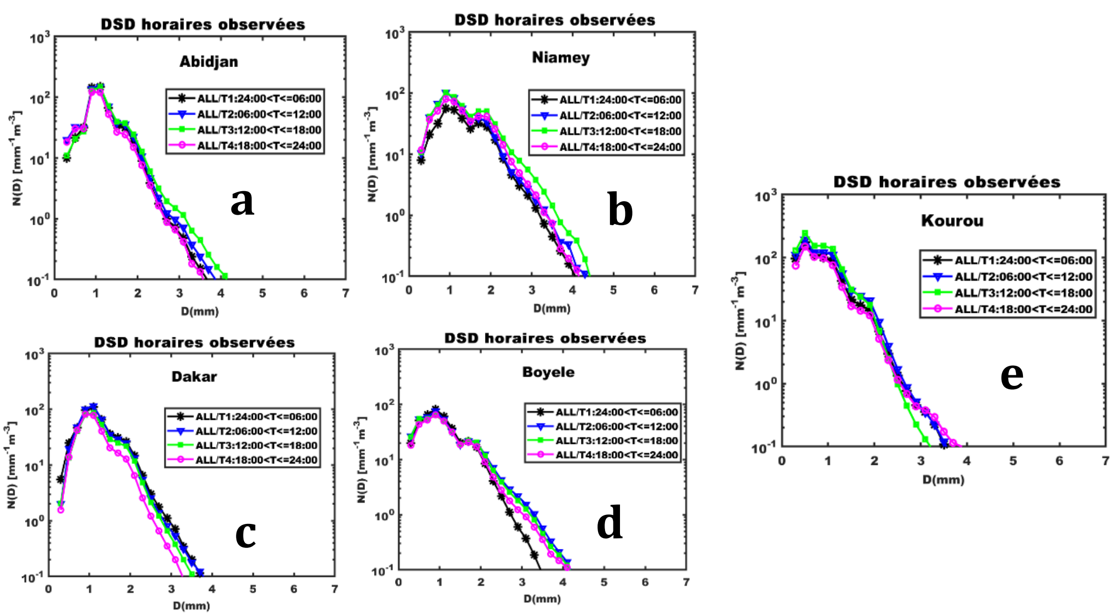

Fig 2 : Shapes of observed diurnal average DSD : (a) Abidjan ; (b) Niamey ; (c) Dakar ; (d) Boyélé ; (e) Kourou

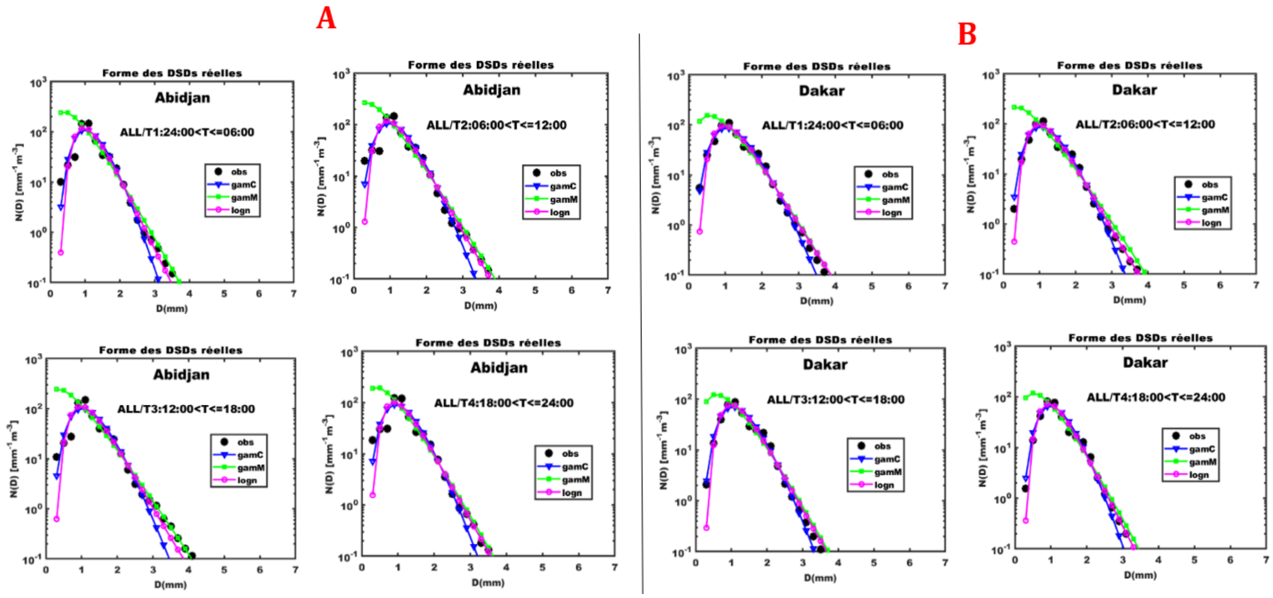

Fig 3-A-B Diurnal average DSD observed and calibrated by model DSD : lognormal (logn) ; complete gamma (gamC) et modified gamma (gamM) : (A) Abidjan ; (B) Dakar.

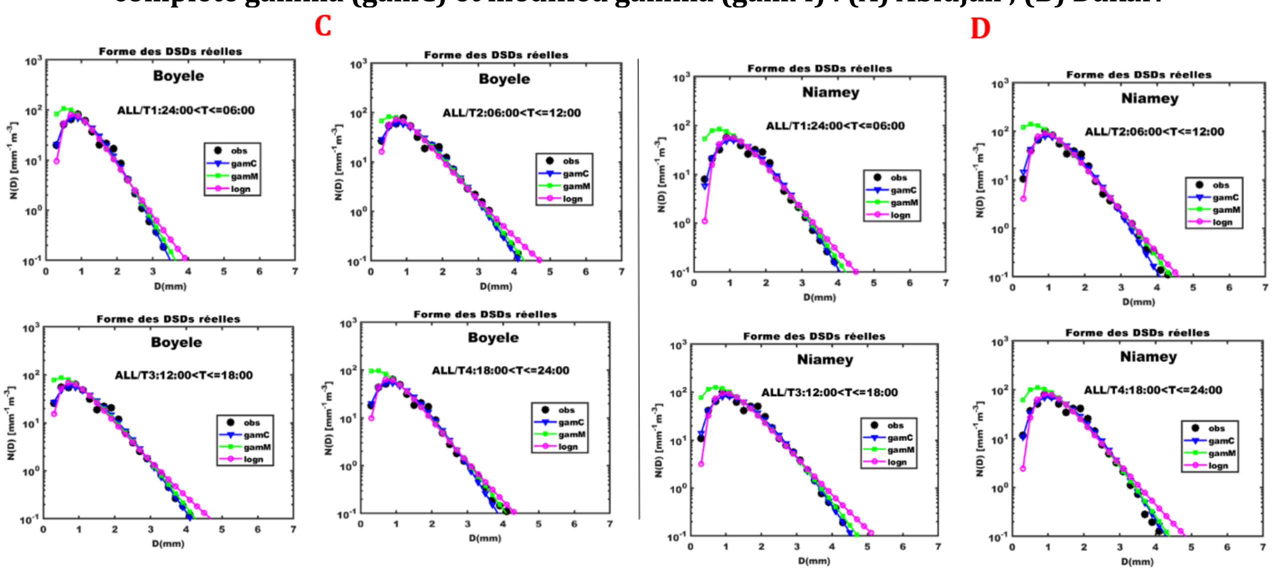

Fig 3-C-D Diurnal average DSD observed and calibrated by model DSD : lognormal (logn) ; gamma complète (gamC) et gamma modifié (gamM) : (C) Boyélé ; (D) Niamey.

E

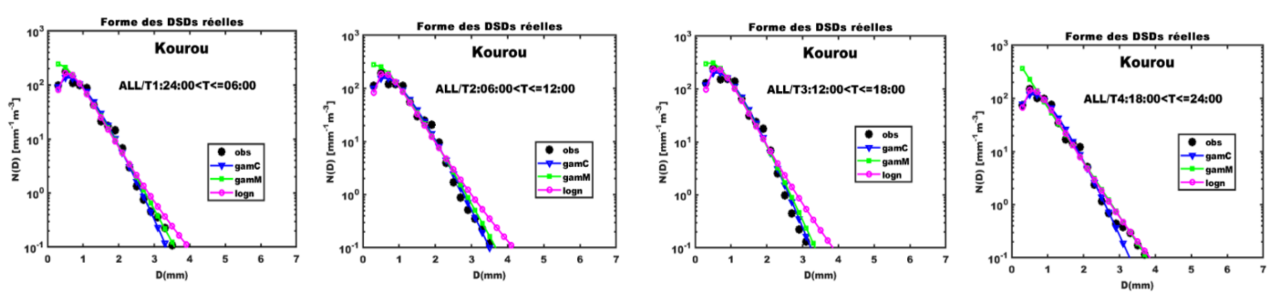

Fig 3-E : Diurnal average DSD observed and calibrated by model DSD : lognormal (logn) ; gamma complète (gamC) et gamma modifié (gamM) : Cas de Kourou.

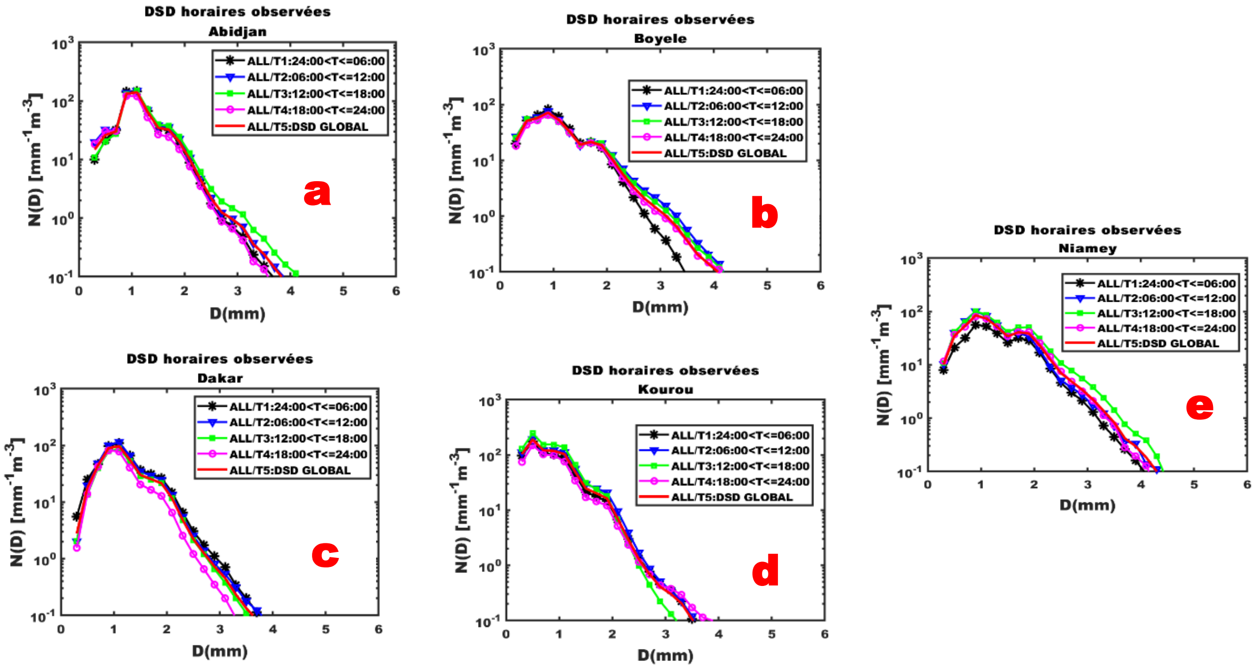

Fig 4 : Overall avarage diurnal DSD subplotted on the four average hourl diurnal studies DSDs : (a) Abidjan ; (b) Boyélé ; (c) Dakar ; (d) Kourou ; (e) Niamey

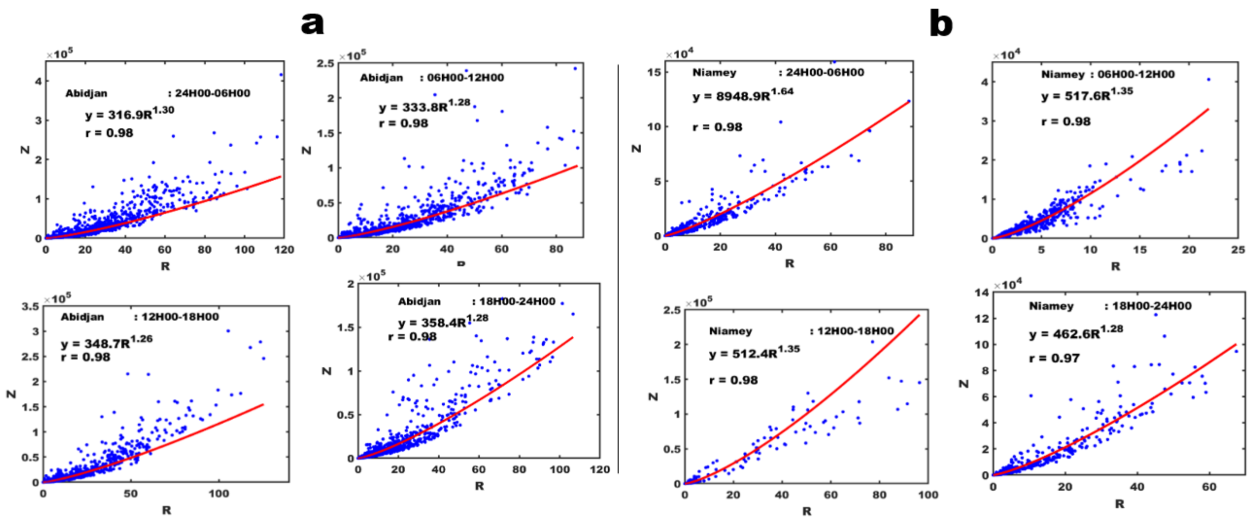

Fig 5-a-b : Diurnal Z-R relations : (a) Abidjan ; (b) Niamey

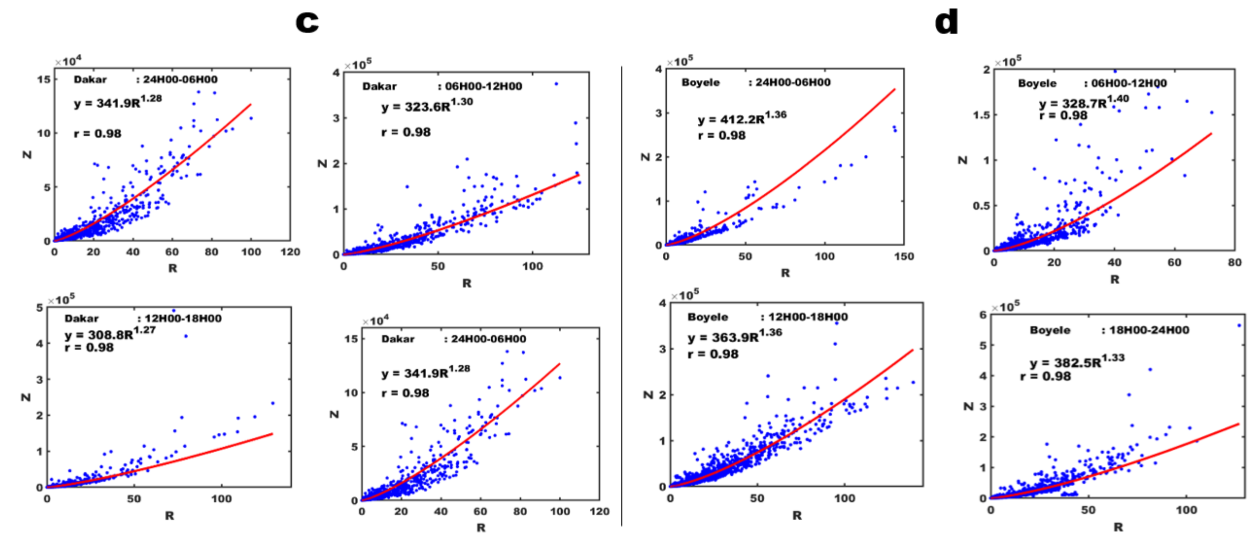

Fig 5-c-d : Diurnal Z-R relations : (c) Dakar ; (d) Boyélé

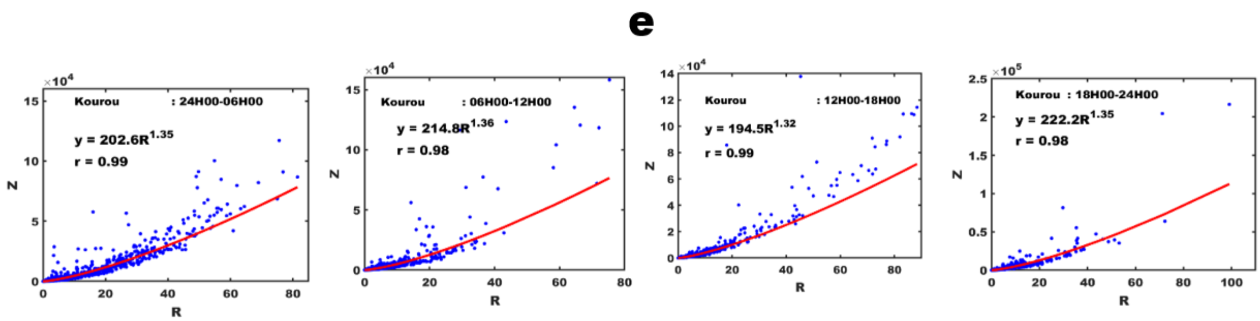

Fig 5-e : Diurnal Z-R relations : Kourou

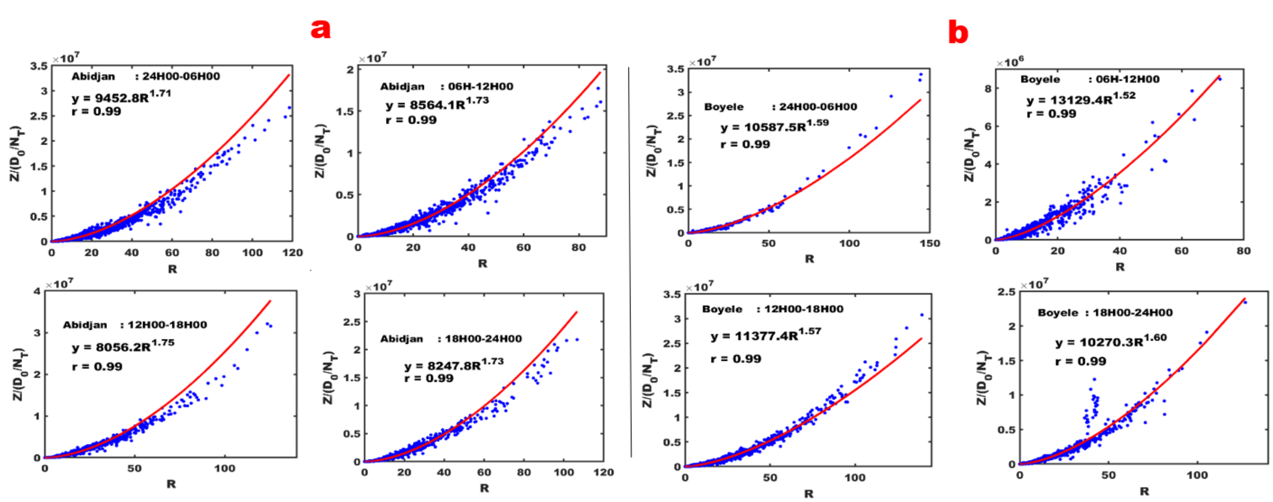

Fig 6-a-b : Scatter plots of ($\frac{Z}{D_0/N_T}$, R) and fitted curves of the four diurnal hourly classes studied : (a) Abidjan ; (b) Boyélé.

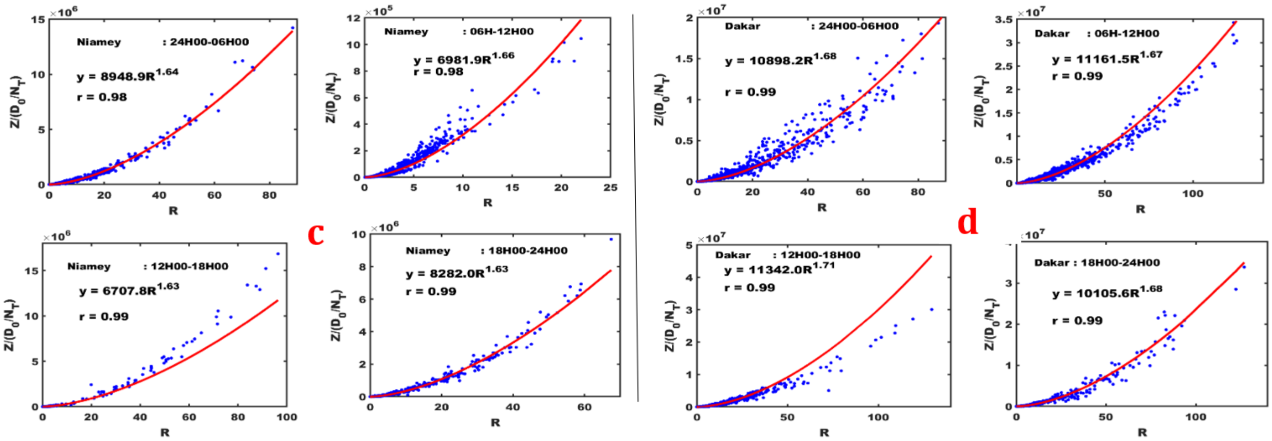

Fig 6-c-d : Scatter plots of ($\frac{Z}{D_0/N_T}$, R) and fitted curves of the four diurnal hourly classes studied : (c) Niamey ; (d) Dakar

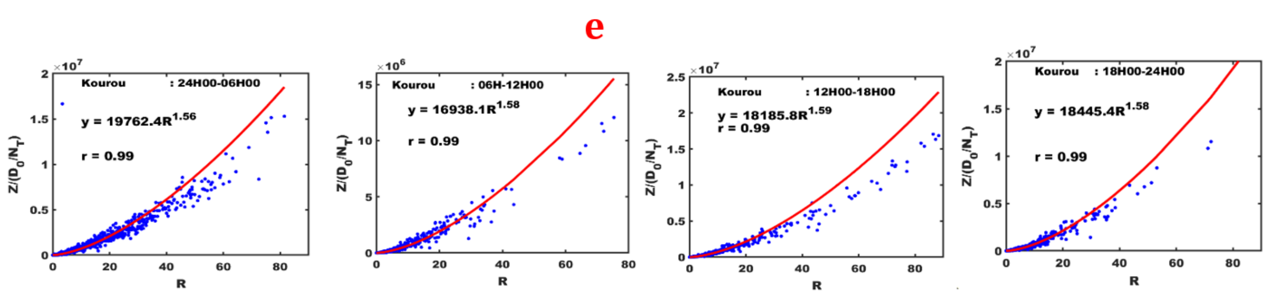

Fig 6-e : Scatter plots of ($\frac{Z}{D_0/N_T}$, R) and fitted curves of the four diurnal hourly classes studied : Cas de Kourou

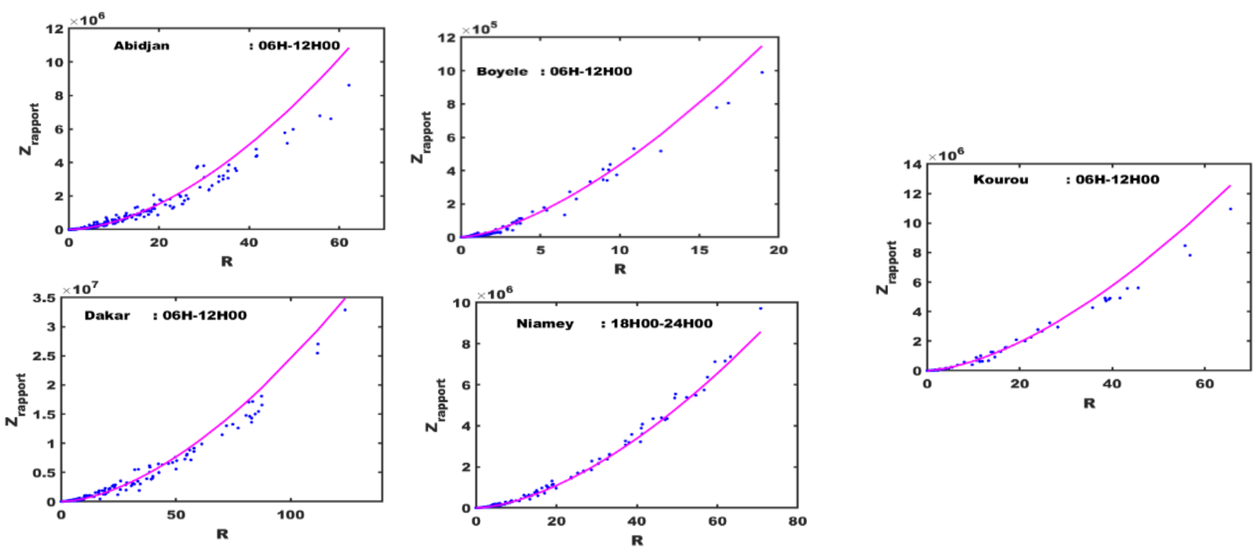

Fig 7: The $Z_{rapport}$-R relationship applied on the scatter plot of validation data for some hourly classes of the studied sites.